

Helium retention and thermal desorption from defects in Fe9Cr binary alloys

T. Zhu ^{a, b}, X. Z. Cao ^{a, *}, S. X. Jin ^a, J. P. Wu ^b, Y. H. Gong ^a, E. Y. Lu ^a, B. Y. Wang ^a, R. S. Yu ^a, L. Wei ^a.

^a Institute of High Energy Physics, Chinese Academy of Sciences, Beijing 100049, China

^b College of Nuclear Technology and Automation Engineering, Chengdu University of Technology, Chengdu 610059, China

Abstract

In order to study the fundamental processes of helium retention and thermal desorption from the structural material of future fusion reactors, thermal desorption measurements were performed to investigate helium trapping from defects in binary Fe9Cr model alloys irradiated by 3 keV and 0.2 keV He ions. Interstitial type dislocation loops, vacancies and vacancy clusters were produced by irradiation with 3 keV helium ions, which acted as the sink trapped the helium atoms. Helium thermal desorption peaks from dislocations, helium-vacancies were obtained by thermal desorption spectroscopy at ~ 540 $^{\circ}$ C, in the range from 205 $^{\circ}$ C to 478 $^{\circ}$ C, respectively. Simple first order dissociation kinetics are used to estimate the activation energies associated with the desorption groups. A sharp desorption peak was observed at ~ 865 $^{\circ}$ C due to the BCC-FCC phase transformation for specimens under all examined implantation conditions.

Keywords: He-ion irradiation, FeCr alloy, Thermal desorption spectroscopy, Defect

1. Introduction

The effect of helium on the microstructure and mechanical properties is one of the most important issues in fusion material research. In nuclear reactor materials, He atoms, generated by a (n, α) reaction, or introduced directly into plasma-facing materials by helium plasma [1, 2], would interact with the irradiation defects, such as dislocations, vacancy clusters, precipitates and even voids. These defects play a

* Corresponding author. Tel.: +86 - 10 - 88233393; E-mail address: caoxzh@ihep.ac.cn (X.Z. Cao)

significant role in the trapping of helium atoms and the prevention of their long-range migration [3]. The interaction between He atoms and defects causes undesirable material degradation such as surface damage, irradiation embrittlement, ductile–brittle transition temperature (DBTT) shift and even the swelling due to the formation of the He bubbles [4].

High-energy particle irradiation will produce the vacancies and interstitial atoms simultaneously in metals. The vacancies aggregate to form clusters, dislocation loops, voids and so on [5]. The aggregating of interstitial atoms also forms the interstitial-type dislocation loops. The defects are diverse and complex under normal irradiation conditions. Thus, it is difficult to distinguish the interaction of any one type of defect with He atoms in metals. However, the dislocation defect could be induced separately by the cold rolling deformation treatment. Low-energy ion irradiation mainly produces the dislocation and vacancy defects [6]. Almost no irradiation defects appeared in metals when the irradiation energy was lower 0.2 keV.

Ferritic-martensitic steels such as Eurofer 97 are recognized as one of the leading candidates for nuclear reactor materials. Such steels, which are based on Fe9Cr, have the advantages of low activation, good swelling resistance and adequate mechanical properties [7, 8]. In the present work, the interaction between He and intentionally-induced dislocations or vacancies in Fe9Cr binary alloys was experimentally investigated by thermal desorption spectroscopy (TDS).

2. Experimental procedures

The samples used in this study were supplied by China Iron & Steel Research Institute Group. Due to heat treatments performed by the manufacturer, the steel is expected to have a tempered martensitic structure.

The bulk materials were first cut to a thickness of 1 mm in 10 mm × 10 mm square sheets and then cold-rolled to a thickness of about 0.2 mm, followed by annealing at 960 °C for 2 h in vacuum ($\sim 10^{-5}$ Pa). To introduce dislocations, well-annealed specimens were cold rolled by 20% at room temperature. Following by annealing at

400 °C for 1 h in a high vacuum was aim to decrease the concentration of vacancies and vacancy clusters, and the main defect was the dislocation in the matrix. The 400 °C annealing treatment cannot remove the dislocation induced by deformation [9]. The specimens were electro-polished to remove possible surface contamination before every annealing treatment.

Helium implantation was carried out using a mono-energetic He ion beam at room temperature (1.2×10^{-6} Pa, in a vacuum). For the 0.2 keV and 3 keV implantations, the beam current was $\sim 1 \mu\text{A}$ and $\sim 3.5 \mu\text{A}$, respectively. The irradiation dose of incident helium ions were $4.2 \times 10^{14} \text{ He/cm}^2$ and $4.2 \times 10^{15} \text{ He/cm}^2$, with a fixed dose rate of about $2.1 \times 10^{13} \text{ He/cm}^2/\text{s}$, as shown in Fig. 1.

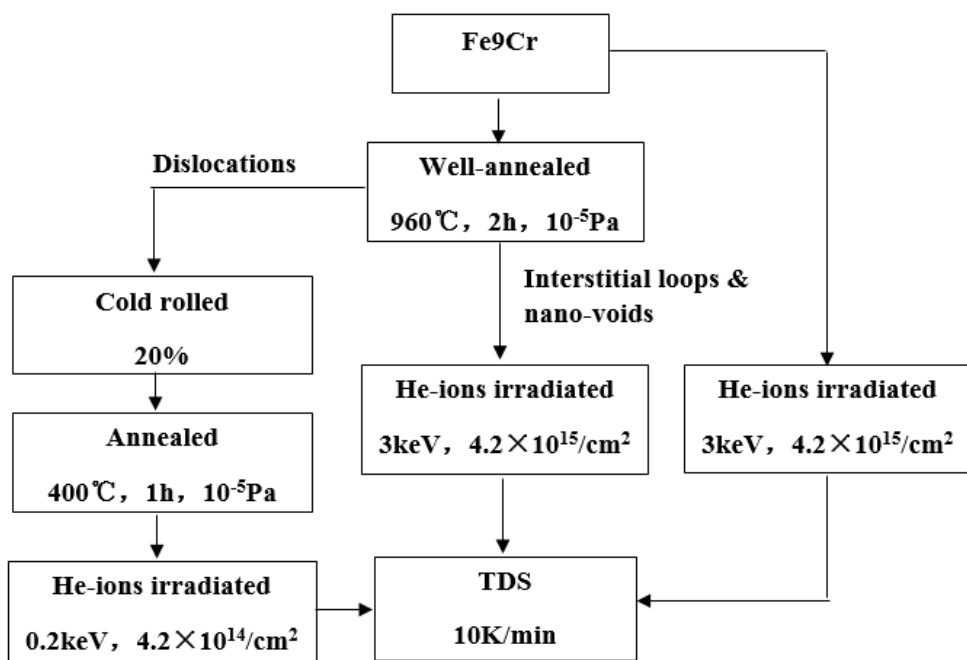


Fig. 1. Preparation of specimens

In the TDS experiments, a quadrupole mass spectrometer was used for the detection of the He atoms, which were released from the linearly heated specimen. The temperature of the sample was measured by a thermocouple. The heating rate (controlled by a PID feedback loop) from RT up to 925 °C was set at 10 °C/min. The level of background signal (at a base pressure of 10^{-7} Pa) is reduced by overnight baking-out of the desorption vacuum chamber at 150 °C. The thermal desorption rate was calibrated by using a standard helium leak source. The desorption sensitivity

coefficient and the minimum detection limit of helium desorption rate are $4.25 \times 10^{21} / \text{A} \cdot \text{s}$ and $2.45 \times 10^9 / \text{s}$, respectively.

3. Results and discussion

The damage, helium distribution, vacancy/He ratio and other factors related to helium ions implantation in Fe9Cr were calculated using SRIM software [10]. For the specimen irradiated by 3 keV He-ions, the vacancy/He ratio is 13. Depth profiles of atomic displacement damage and helium concentration are shown in figure 2. It shows that He-ions mainly distributed in the region from 0 to 50 nm and peaked at about 15 nm. The irradiation induced defects peaked at about 7 nm, which is similar to the distribution of implanted He-ions.

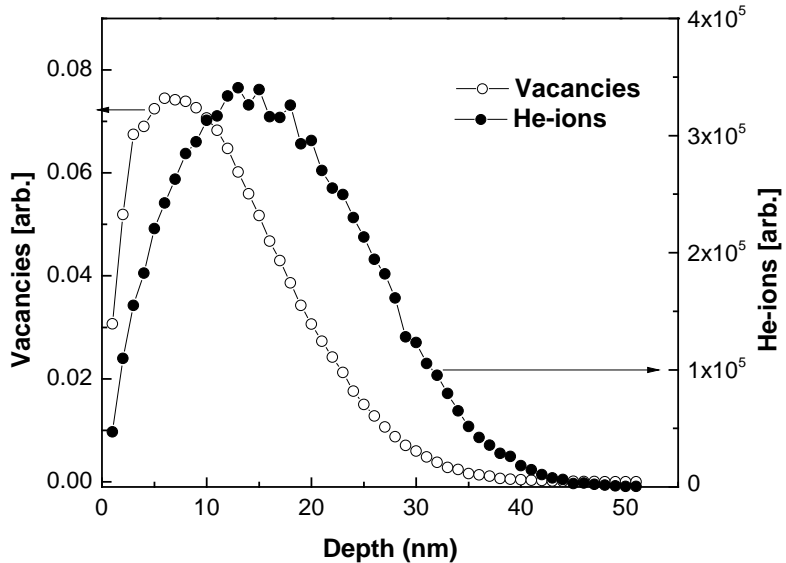


Fig. 2. Depth profiles of irradiation damage and He concentration for Fe9Cr irradiated by 3 keV He-ions.

Helium thermal desorption spectra are shown in Figs. 3-5. Fig. 3 shows the desorption spectra for the cold rolling specimen (containing mainly dislocations) irradiated by 0.2 keV helium ions to a dose of $4.2 \times 10^{14} \text{ He/cm}^2$. The desorption spectra in Fig. 4 is the well-annealed specimen irradiated by 3 keV helium ions to $4.2 \times 10^{15} \text{ He/cm}^2$. The desorption spectra in Fig. 5 is from a raw specimens after implantation by 3 keV helium ions to $4.2 \times 10^{15} \text{ He/cm}^2$. The desorption event for the cold rolling

specimen irradiated by 0.2 keV helium ions to $4.2 \times 10^{14} \text{ He/cm}^2$ started from room temperature to 925 °C. There were four groups appeared in Fig. 3, as follows: Group A1 from 210 °C to 315 °C, the peak at 290 °C, group A2 from 315 °C to 400 °C, the peak at 375 °C, group A3 from 400 °C to 670 °C, the peak at 540 °C, and group A4 at 865 °C. Here the word ‘Group’ is used instead of ‘Peak’ because each ‘Group’ requires more than one single dissociation event to reasonably reproduce the peak width and thus, may involve multiple dissociation mechanisms [11]. Fig. 4 presents three groups in the helium thermal desorption spectra, group B1 from 205 °C to 395 °C, group B2 from 420 °C to 580 °C, and group B3 from about 580 °C to 900 °C, the peaks at 340 °C, 540 °C and 865 °C, respectively. As could be seen in Fig. 5, the peaks in the spectra were classified into groups C1, C2, and C3. Group C1 lies on the low temperature side, spanning from 195 °C to 478 °C, group C2 in the intermediate temperature range, from 478 °C to 580 °C, and group C3 in the high temperature range, from 580 °C to 910 °C, the peaks at 410 °C, 530 °C and 865 °C, respectively.

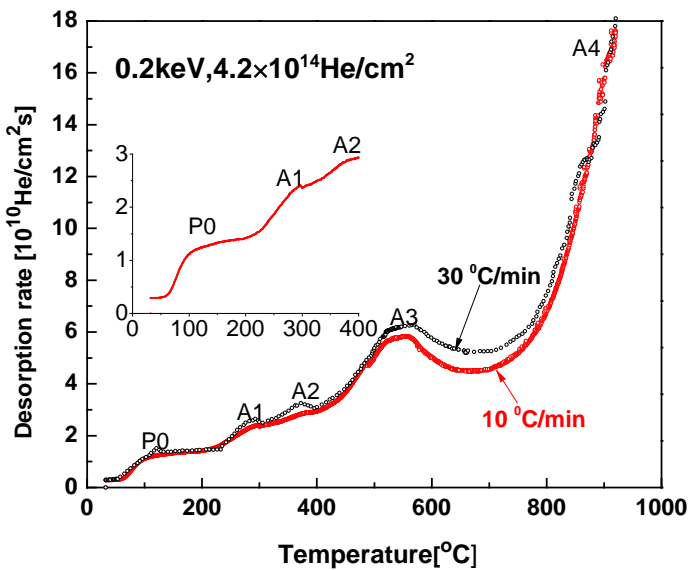


Fig. 3 Desorption spectra in cold rolling specimen implanted by 0.2 keV helium ions to $4.2 \times 10^{14} \text{ He/cm}^2$

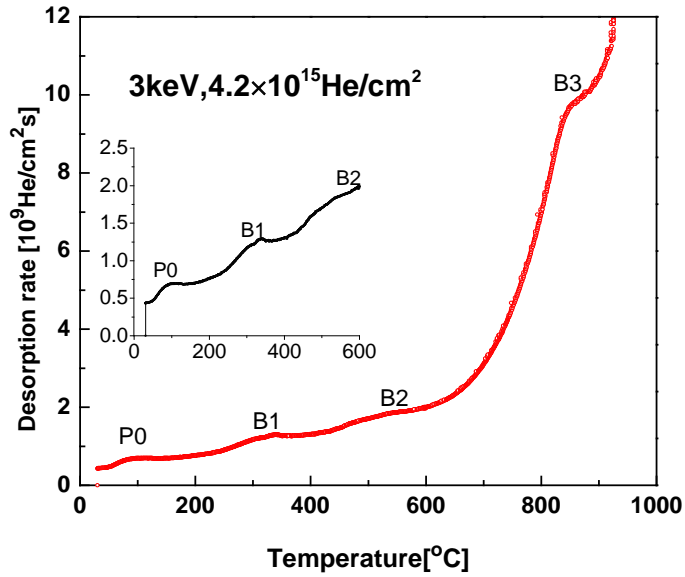


Fig. 4 Desorption spectra in a well-annealed specimens irradiated by 3 keV helium ions to $4.2 \times 10^{15} \text{ He/cm}^2$.

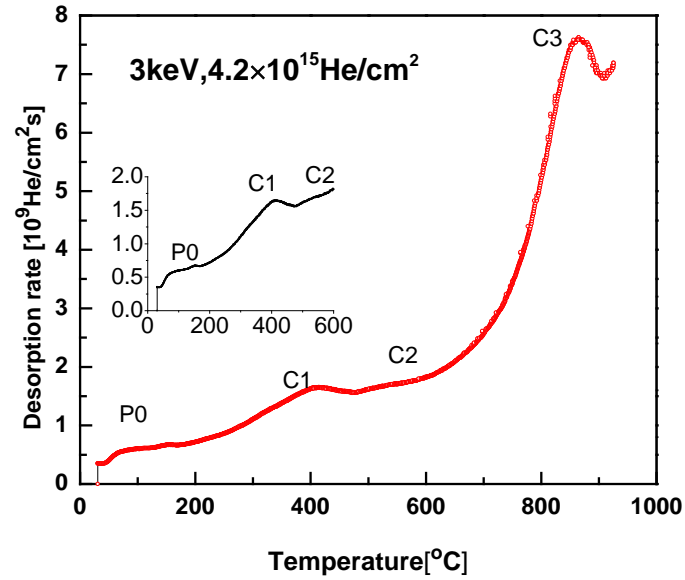


Fig. 5 Desorption spectra in a raw specimen after implantation by 3 keV helium ions to $4.2 \times 10^{15} \text{ He/cm}^2$.

The helium desorption peaks with a constant heating rate correspond to the release of helium atoms from different trapping sites [12]. The desorption activation energy were calculated based on simple first order dissociation kinetics, i.e.:

$$dN/dt = -k_0 N \exp(-E/k_B T), \quad (1)$$

Where N is the remaining number of helium atoms, and not yet desorb from a specific trap, k_0 is the jumping frequency (usually on the order of $10^{13}/\text{s}$), E is the activation energy for the trap, and k_B is the Boltzmann constant. The relationship among desorption peak temperature T_p (in K), heating rate β and activation energy E was derived as follows [11, 13]:

$$\ln\left(\frac{\beta}{T_p^2}\right) = -\frac{E}{k_B T_p} + \ln\left(\frac{k_0 k_B}{E}\right), \quad (2)$$

In order to define experimentally both the jumping frequency and activation energy, the ramping measurement was also performed at a heating rate of $30\text{ }^\circ\text{C}/\text{min}$, which shifted the temperature of peak A3 to $564\text{ }^\circ\text{C}$, as shown in Fig. 3. Therefore, the use of two sets of T_p vs. β value can determine both the activation energy E and the jumping frequency k_0 . In this case, we obtain $E = 2.54\text{ eV}$ and $k_0 = 3.9 \times 10^{13}/\text{s}$. As the heating rate β was fixed at $10\text{ }^\circ\text{C}/\text{min}$, the activation energy (in electron volts) for an average group of traps was estimated as the follows:

$$E = 0.0031T - 0.056, \quad (3)$$

It should be noted that this simple model has assumed that there are no mutual transformations among traps with different E values, which is certainly not the real case since evolution among different traps/defect-clusters with distinct E values is unavoidable. However, this simple model can provide an estimate for the average E values of a group of traps which have mutual transformation among themselves and yet sufficiently separated from other groups with respect to E values. The desorption energies of helium atoms from defects were estimated by Eq. (3). These were 1.69 eV for peak A1, 1.95 eV for peak A2, and 2.50 eV for peak A3, 1.84 eV for peak B1, 2.46 eV for peak B2, 2.06 eV for peak C1, 2.43 eV for peak C2, and 3.47 eV for peak A4, B3 and C3.

The helium desorption peak, Peak A3, was likely assigned to dissociation from dislocation networks (He_nD). Single vacancies and dislocations are known to be induced by cold rolling. However, mainly the dislocation existed in specimen after annealing at $400\text{ }^\circ\text{C}$, and most of the single vacancies were eliminated by annealing at $400\text{ }^\circ\text{C}$ [5]. Both the desorption temperature for the B2 in Fig. 4 and C2 in Fig. 5 was

~540 °C, and the desorption activation energies of helium atoms from B2 and C2 were 2.46 eV and 2.43 eV, respectively. Very likely the B2 and C2 peaks were similar with A3 and assigned to dissociation from dislocation networks (He_nD). The defect corresponding to B2 was the interstitial-type dislocation induced by 3 keV helium ions irradiation, and the defect for C2 was the pre-existing dislocation. In the reduced activation ferritic (RAF) steels and 9Cr-ODS steels, Kimura et al. assigned helium desorption at 550 °C to He_nD [14]. Ono et al. explained that the peak at 547 °C are attributed to a release of helium by annihilation of loop dislocation segments owing to glide in Fe9Cr ferritic alloy [15]. Peak B1 was assigned to the dissociation from the vacancies (He_nV_m) formed by 3 keV helium ion irradiation. The pre-existing vacancies have been eliminated due to the 960 °C annealing treatment in the specimen before the He implantation. The dissociation energy of peaks A2 and C1 was 1.95 eV and 2.06 eV, respectively, which is close to the data of the peak B1 (1.84 eV). Thus, the peaks A2 and C1 were contributed mainly by the dissociation from vacancies. However, the vacancy for A2 was induced by cold rolling and the vacancy in Fig. 5 was the pre-existing vacancies and irradiation vacancies. Peak A1 was detected in the temperature range of 210-315 °C, helium desorption in this temperature range is attributed to the release of helium trapped at single vacancy [16]. This is qualitatively consistent with the results of helium in iron reported by Morishita et al., Group from 250 to 380 °C can be ascribed to helium desorbing from a vacancy in the neighbourhood of surface, as well as from overpressurized species He_nV_m [17]. Desorption in the range from 430 to 520 °C corresponds to helium desorbing from multiply-filled vacancies (He_nV, 2 ≤ n ≤ 6) [15, 18, 19, 20]. In addition, a group (P0) was detected in the temperature range of 40-80 °C for each of the spectra, and the trapping sites for the peak were likely a result of a combination of surface contamination and oxidation [18].

There have been numerous theoretical studies attempting to define activation energy mechanism [21-25]. According to the traditional definition, the activation energy is a combination of the binding and migration energies of a helium atom and a defect. In the present study, the desorption energies of helium atoms from dislocations, helium-vacancies were estimated by a simple first order dissociation kinetics, 2.50 eV, in the

range from 1.69 to 2.06 eV, respectively, and it is in good agreement with the one obtained theoretically by Wang et al. [22], Ortiz et al. [21]: namely, 2.58 eV, 1.84 eV.

One general feature of the desorption spectra can be noticed in Figs. 3-5, which is the desorption peak induced by alpha-gamma (BCC-FCC) phase transition. In Fig. 5, there exists a sharp peak (see the C3) for the desorption spectra in a raw specimen irradiated with 3 keV helium ions to 4.2×10^{15} He/cm², and the peak was at ~ 865 °C. The C3 peak is associated with the alpha-gamma (BCC-FCC) phase transition [11, 15]. The similar peaks, peak B3 and A4 seated at ~ 865 °C, could also be seen in Figs. 3 and 4, respectively. In the present work, we did not analyze the desorption signal at even higher temperatures since we were mainly interested in helium behavior in BCC iron.

In the range of 25 °C - 925 °C, the total desorption amount of helium in Fig. 3 was approximate 10 times larger than that in Figs 4 and 5, and the total desorption amount in Fig. 4 was similar with that in Fig. 5. Therefore, this indicates that total amount of helium desorption is associated with implantation energy and dose [18].

4. Conclusions

In the present work, the helium desorption behavior from the Fe9Cr binary alloys was investigated by TDS. 3 keV He ion irradiation could introduce the vacancy and dislocation defect. The cold rolling deformation and the subsequent 400 °C annealing treatment could also induce the mainly dislocation defects. These defects, acted as the trapping sites, could capture the helium atoms. Helium thermal desorption peaks from dislocations, helium-vacancies were obtained by TDS at ~ 540 °C, in the range from 205 °C to 478 °C, respectively. According the relation between defects and desorption temperature, the desorption energies of helium atoms from defects were estimated and analyzed. The phase transition for alpha-gamma (BCC-FCC) in Fe9Cr alloy would release the helium atoms, and the desorption temperature was about at 865 °C.

Acknowledgments

This work is supported by the National Natural Science foundation of China [grant number 11475193, 91226103, 11475197, 11575205 and 11505192].

References

- [1] D. Kaminsky, S.K. Das, *J. Nucl. Mater.* 76-77 (1978) 256.
- [2] R.E. Stoller, *J. Nucl. Mater.* 174 (1990) 289.
- [3] T. Kawakami, K. Tokunaga, N. Yoshida, *Fusion Eng. Des.* 81 (2006) 335.
- [4] V.N. Chernikov, A.P. Zakharov, P.R. Kazansky, *J. Nucl. Mater.* 155-157 (1988) 1142.
- [5] Q. Xu, T. Ishizaki, K. Sato, T. Yoshiie, S. Nagata, *Mater. Trans.* 47 (2006) 2885.
- [6] X.Z. Cao, Q. Xu, K. Sato, T. Yoshiie, *J. Nucl. Mater.* 412 (2011) 165.
- [7] S.J. Zinkle, N.M. Ghoniem, *J. Nucl. Mater.* 417 (2011) 2.
- [8] A. Kohyama, A. Hishinuma, D.S. Gell, R.L. Klueh, W. Diets, K. Ehrich, *J. Nucl. Mater.* 233–237 (1996) 138.
- [9] K. Sato, T. Yoshiie, T. Ishizaki, Q. Xu, *Phys. Rev. B* 75 (2007) 094109.
- [10] J.F. Ziegler, J.P. Biersack, U. Littmark, *The Stopping and Range of Ions in Matter*, Pergamon, New York, 1984.
- [11] D. Xu, B.D. Wirth, *J. Nucl. Mater.* 386-388 (2009) 395.
- [12] E.V. Kornelsen, A.A. van Gorkum, *Vacuum* 31 (1981) 99.
- [13] K. Morishita, R. Sugano, B.D. Wirth, T. Diaz de la Rubia, *Nucl. Instum. Methods. Phys. Res. B* 202 (2003) 76.
- [14] A. Kimura, R. Sugano, Y. Matsusshita, S. Ukai, *J. Phys. Chem. Solids* 66 (2005) 504.
- [15] K. Ono, K. Arakawa, H. Shibasaki, H. Kurata, I. Nakamichi, N. Yoshida, *J. Nucl. Mater.* 329-333 (2004) 933.
- [16] Morishita K, Sugano R, Iwakiri H, Yoshida N and Kimura A 2001 Proc. 4th Pacific Rim Int. Conf. on Advanced Materials and Processing (Hawaii) 1-2 1395.
- [17] K. Morishita, R. Sugano, *J. Nucl. Mater.* 353 (2006) 52.
- [18] R. Sugano, K. Morishita, H. Iwakiri, N. Yoshida, *J. Nucl. Mater.* 307-311 (2002) 941.
- [19] K. Morishita, R. Sugano, H. Iwakiri, N. Yoshida, A. Kimura, *PRICM* 4 (2001) 1395.
- [20] R. Sugano, K. Morishita, A. Kimura, H. Iwakiri, N. Yoshida, *J. Nucl. Mater.* 329-

333 (2004) 942.

[21] C.J. Ortiz, M.J. Caturla, C.C. Fu, F. Willaime, Phys. Rev. B 75 (2007) 100102.

[22] Y.X. Wang, Q. Xu, T. Yoshiie, Z.Y. Pan, J. Nucl. Mater. 376 (2008) 133.

[23] C.C. Fu, F. Willaime, Phys. Rev. B 72 (2005) 064117.

[24] D. Xu, B.D. Wirth, Fusion Sci. Technol. 56 (2009) 1064.

[25] D. Xu, B.D. Wirth, J. Nucl. Mater. 403 (2010) 184.